scientific reports

Check for updates

OPEN

Source apportionment of soil heavy metals with PMF model and Pb isotopes in an intermountain basin of Tianshan Mountains, China

Tao Zeng[1,2,3], Long Ma[1,2,3]✉, Yizhen Li[1,2,3], Jilili Abuduwaili[1,2,3], Wen Liu[1,2,3] & Sen Feng[1,2,3]

A boom in tourism may lead to the enrichment in heavy metals (HMs) in soils. Contamination with HMs poses a significant threat to the security of the soil environment. In this study, topsoil samples were collected from a tourist area of Sayram Lake, and the concentrations of HMs (Cr, Cu, Ni, Pb, Zn and Cd) were determined. With contamination and eco-risk assessment models, correlation analysis, Pb isotope ratios, redundancy analysis and positive matrix factorization (PMF) model, the risks and sources of HMs in the soil were studied. The I_{geo} results suggested that Cd was the primary pollutant in the tourist area of Sayram Lake. The potential ecological risk index (PERI) showed that the study area was at low risk, and the pollution load index (PLI) indicated that the study area had a moderate contamination level. Qualitative and quantitative analyses apportioned three sources of HMs, namely, natural sources (38.5%), traffic sources (27.2%) and mixed sources (tourist waste and atmospheric deposition) (34.3%). Redundancy analysis results showed that the HMs content was related to SiO_2, Al_2O_3, TiO_2, P_2O_5, MnO, K_2O, Fe_2O_3 and SOC, and heavy metals tended to be stored in soil particles of grain sizes < 32 µm. These findings are expected to provide useful insights into the source identification of HMs in the soils of mountain tourism areas and provide a scientific decision-making basis for sustainable tourism development and for the assessment of ecological service values in the Tianshan Mountains.

Over the past decades, the impact of human activities such as the exploitation of mineral resources[1], agricultural irrigation[2], industrial development[3], tourism and urban infrastructure[4,5], and road transportation[6] has led to a significant enrichment in heavy metals (HMs) in soils. Excessive amounts of HMs in the soil environment can disrupt soil functions[7] and cause risks to human health through ingestion, inhalation and dermal contact[8]. For example, Pb, Cd and Hg can cause damage to the human nervous system and kidneys, Cu can cause neurological problems and liver disease, and Ni can inhibit the development of immune organs by inducing excessive apoptosis and inhibiting cell proliferation[9]. The risks posed by HMs to human health and terrestrial ecosystems have attracted widespread attention, and HMs have been listed as priority pollutants for monitoring[10]. Therefore, a systematic study of HMs in the soil environment is of great importance for maintaining ecological security and human health.

Mountains are the starting point for materials circulation and energy flow in global ecosystems, and they are sensitive to global climate and environmental change[11]. Due to the vulnerability and sensitivity of the mountain ecological environment in arid areas, mountain systems are more likely to respond to external environmental changes, and soil contamination in mountain areas by HMs can reduce the service functions and values of mountain ecosystems and even pose threats to human health[12]. The rapid urbanization and industrialization that has occurred in recent decades have accelerated the accumulation of HMs in the environment[13]. Although mountainous areas are far from urban industrial centers that release HMs, the barrier effect and condensation effect of mountainous areas induce the deposition of HMs discharged from industries into mountainous soils through long-distance atmospheric transport[14], making environmental safety issues increasingly prominent[15]. Scientific publications have shown that the development of transportation[16] and tourism[17,18] has also become a key factor in the enrichment of HMs in some mountainous areas. These results demonstrate that the sources of

[1]State Key Laboratory of Desert and Oasis Ecology, Xinjiang Institute of Ecology and Geography, Chinese Academy of Sciences, Ürümqi 830011, China. [2]Research Center for Ecology and Environment of Central Asia, Chinese Academy of Sciences, Ürümqi 830011, China. [3]University of Chinese Academy of Sciences, Beijing 100049, China. ✉email: malong@ms.xjb.ac.cn

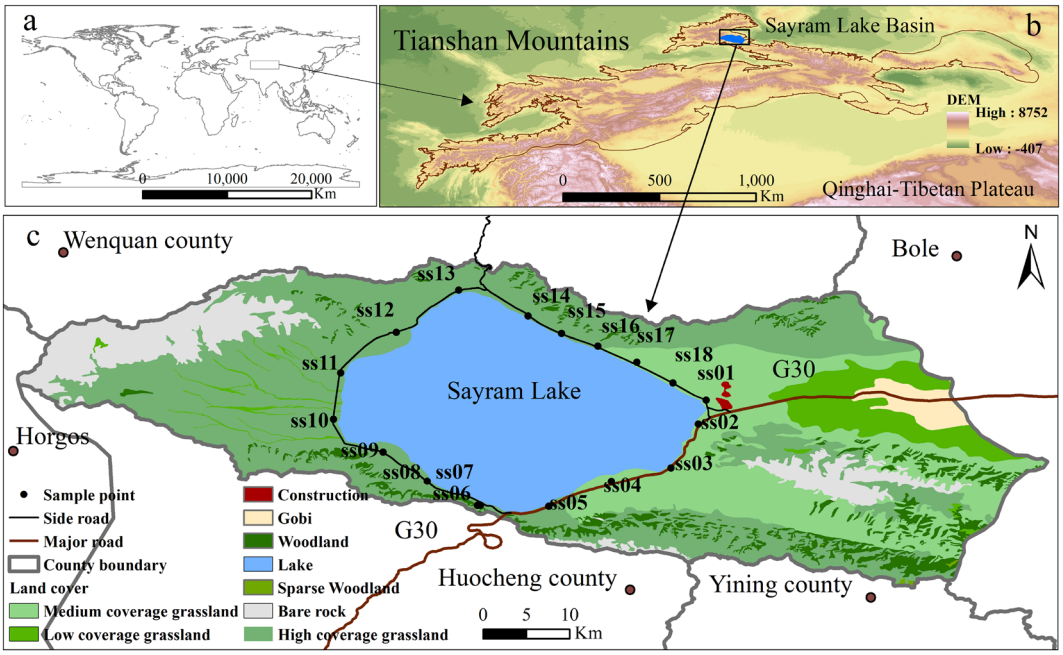

Figure 1. Location map and distribution of sampling points for the Sayram Lake Basin. The graphs (**a**, **b**) and (**c**) were generated by QGIS 3.26.3 (https://www.qgis.org) with the global vector data from the GADM database (https://gadm.org), the DEM data from the Natural Earth database (https://www.naturalearthdata. com), and the land use data from the Resource and Environmental Science and Data Center database (https://www.resdc.cn). The combination of graphs (**a**, **b**) and (**c**) was accomplished with linkscape 1.2.1 (https://inkscape.org).

HMs in mountain soils are diverse; therefore, quantitative and qualitative analyses of the sources of soil HMs are particularly significant for precisely controlling pollution sources[19]. Presently, many quantitative methods are widely applied to identify sources of soil HMs, such as the PMF model[20], principal component model analysis/multiple linear regression (PCA/MLR)[21], UNMIX model[22], and chemical mass balance method (CMB)[23]. Qualitative methods such as PCA, correlation analysis and cluster analysis cannot provide the contributions of pollution sources to HMs. Additionally, the stable isotopic compositions of HMs have an excellent tracing capacity, and stable isotopes of Pb, Zn, Cd, and Cu have been widely used for contamination source identification[23,24]. In the above approaches, PMF is a receptor model recommended by the U.S. Environmental Protection Agency (US EPA) for pollutant source apportionment, which takes into account the uncertainty of the data matrix and provides contributions of pollutant sources to HMs under nonnegative constraints[25]. The PMF model has been applied to source apportionment research of pollutants in the atmosphere, sediment and soils[26,27] and has achieved positive results. Receptor models combined with isotopes are expected to be an efficient way to identify HM sources when multiple HMs coexist.

The Sayram Lake Basin (Fig.1) is located in the middle of the West Tianshan Mountains in Xinjiang, which is a typical, closed watershed of the Tianshan Mountains. In recent decades, with economic development, tourism and transportation industries have rapidly emerged. As a 5A-level tourist attraction, the tourism area of Sayram Lake receives 2,530,000 tourists annually (http://www.xjboz.gov.cn/), which may cause high-intensity traffic problems and generate large amounts of tourist wastes, which lead to negative effects on the environment. However, these problems have not received sufficient attention. Existing studies on the Tianshan Mountains have focused on climate change and water resources[28,29], land use and land cover[30], snow and glaciers[31], and paleolimnology[32]. The lack of research on the concentration, contamination and eco-risk characteristics of HMs and their influencing factors in the Tianshan Mountains has significantly affected the development of agriculture and pastoralism, tourism value evaluations and identifications of the ecological security of this region.

Thus, an investigation was carried out on the topsoil of the tourist area of Sayram Lake. The main objectives of this work were (1) to reveal the concentration characteristics of HMs; (2) to assess the degree of contamination and eco-risk of HMs; and (3) to identify the potential sources and contributions of soil HMs based on the PMF model and Pb isotope ratios. The results of the study are expected to provide scientific support for the prevention and control of HM pollution, for the sustainable development of the ecological environment and for the evaluation of ecological service values of mountain areas.

Results

Whole-rock geochemical compositions and grain-size characteristics. The whole-rock composition results are shown in Table S1, and the statistical characteristics are shown in Fig. 2. In general, the concentration range (%) and mean value (%) of the whole-rock composition in the topsoil of the tourist area of Sayram Lake decreased in the following order: SiO_2 (34.8–62.09, 51.69) > LOI_{1000} (8.57–25.83, 16.02) > Al_2O_3

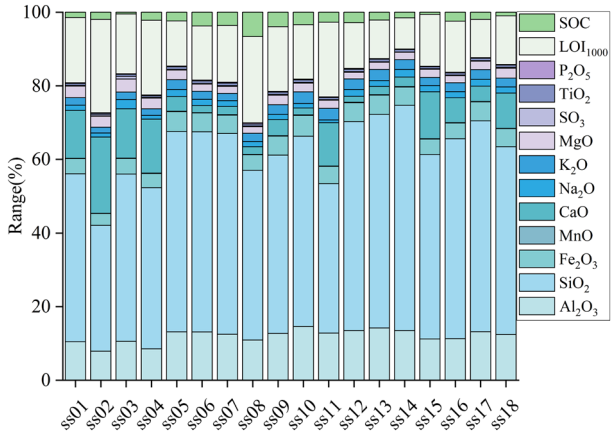

Figure 2. Whole-rock composition results of each sampling point in in the tourist area of Sayram Lake.

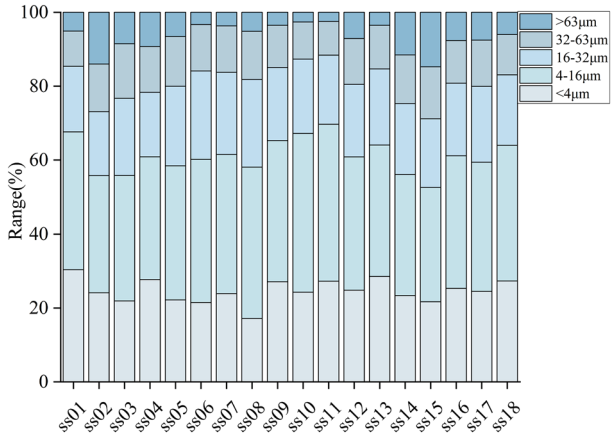

Figure 3. The grain-size composition of the topsoil in the tourist area of Sayram Lake.

(7.99–15.18, 12.33) > CaO (1.71–21.10, 7.35) > SOC (2.61–10.50, 5.17) > Fe_2O_3 (1.6–3.3, 4.8) > K_2O (1.6–3.33, 2.50) > MgO (1.85–3.57, 2.44) > Na_2O (0.79–2.51, 1.61) > TiO_2 (0.41–0.72, 0.61) > SO_3 (0.10–0.73, 0.23) > P_2O_5 (0.14–0.35, 0.20) > MnO (0.06–0.15, 0.11).

The grain-size composition characteristics of the topsoil samples are shown in Fig. 3. According to the Udden-Wentworth classification[33], the soil grain size was divided into five classes: clay (< 4 μm), fine-silty (4–16 μm), silty (16–32 μm), coarse-silty (32–64 μm) and sandy (> 64 μm). The percentage of grain-size composition of each level from large to small was fine-silty (36.49%) > clay (24.64%) > silty (19.98%) > coarse-silty (12.11%) > sandy (6.78%).

Heavy-metal concentrations and Pb isotope ratios. The descriptive statistics for Cr, Cu, Ni, Pb, Zn and Cd in the topsoil of the tourist area of Sayram Lake are shown in Table S2, and the statistical characteristics are shown in Fig. 4. The highest concentration of HM was that of Zn, which ranged from 62–141 mg/kg, and the mean value was 101 mg/kg. The lowest concentration of HM was that of Cd, which ranged from 0.2–1.08 mg/kg, with an average value of 0.34 mg/kg. The average concentrations of Cr, Cu, Ni and Pb were 53.5 mg/kg, 27.48 mg/kg, 27.89 mg/kg and 24.59 mg/kg, respectively. Additionally, the average Pb and Zn concentrations exceeded the background values by 33% and 50%, respectively. The mean concentration of Cd was 2.8 times that of the background value (0.12 mg/kg). Furthermore, the CVs of Cd, Pb and Zn were 0.58, 0.26 and 0.2, respectively, while the CVs of the other elements were less than 0.2. These results demonstrated that Cd, Pb and Zn had strong variability in their mean values, and the variability in Cd was most significant.

The descriptive statistics of the Pb isotope ratios ($^{206}Pb/^{207}Pb$ and $^{208}Pb/^{206}Pb$) in the topsoil of the tourist area of Sayram Lake are shown in Table S2. The results showed that $^{206}Pb/^{207}Pb$ ranged from 1.09 to 1.21, with an average value of 1.15. $^{208}Pb/^{206}Pb$ ranged from 2.01 to 2.18, with an average value of 2.11.

Contamination and eco-risk evaluation of HMs. The accumulation of HMs in soils may have a negative impact on the ecological environment. Therefore, researchers evaluate the effects of HMs on the environment based on a certain system of evaluation criteria and corresponding mathematical models. A single evalu-

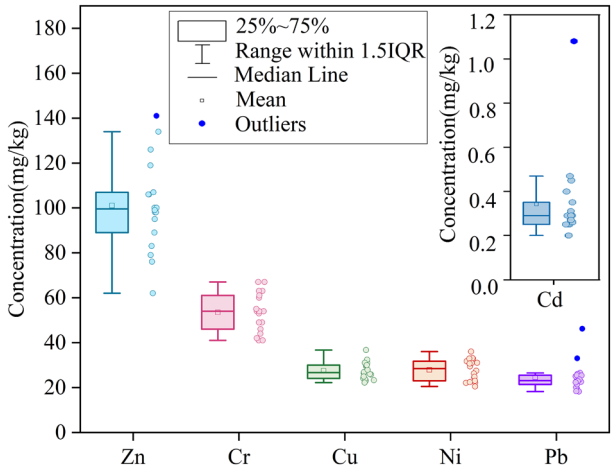

Figure 4. Concentrations of HMs in the topsoil of the study area.

ation method may lead to errors in the results, so multiple evaluation criteria (I_{geo}, PERI and PLI) were applied to evaluate the topsoil in the tourist area of Sayram Lake to strengthen the credibility of the assessment results.

The average I_{geo} values of HMs in the topsoil of the tourist area of Sayram Lake decreased in the following order: Cd (0.80) > Zn (−0.03) > Cu (−0.19) > Pb (−0.21) > Ni (−0.44) > Cr (−0.70). From the average value of I_{geo}, the area was slightly contaminated with Cd (0.8), and the average value of I_{geo} of the other elements was less than 0, showing no contamination. From a more microscopic point of view, 22.2% of all sample points were moderately Cd-contaminated, these points were concentrated in the southeast of the study area (ss04, ss05, ss06, ss07), and the rest of the sample points were slightly contaminated. For Pb, there were two sample points with moderate contamination, and the I_{geo} of the remaining points was less than 0. For Zn, 39% of the samples were slightly contaminated. The I_{geo} values of Cr, Ni and Cu were less than 0, indicating that these HMs caused no contamination of the tourist area of Sayram Lake.

E^{i}_{r} can indicate the risk of individual HMs. Referencing the grading criteria for E^{i}_{r}, Cr, Cu, Ni, Pb and Zn showed values of E^{i}_{r} that did not exceed 40, indicating that they posed low risks. The mean E^{i}_{r} of Cd was 85.69, which indicated a considerable risk. The PERI of Cd ranged from 67.39 to 295.80, with only one sample site (ss04) having a PERI (295.80) greater than 150, which was a moderate ecological risk area. The PLI ranged from 1.04 to 1.89, suggesting a moderate contamination level in the tourist area of Sayram Lake.

Discussion

The plots of I_{geo}, PERI, and PLI of HMs in the topsoil of the tourist area of Sayram Lake (Fig. 5) reveal the degree of HM pollution and eco-risk in this study area on the one hand and, on the other hand, indicate the direction for the relevant agencies to target soil environmental protection and HM pollution prevention and control measures. In this study, the I_{geo} results showed that Cd was the most highly enriched HM, and Pb, Zn, Cd, and Ni were slightly enriched in a few sample sites. The unnatural accumulation of these elements is usually closely associated with human activities in the area[34]. Tourism is the main economic activity in the district, and published studies have reported that tourism infrastructure construction (e.g., roads, buildings, etc.) and tourism wastes (e.g., plastic bags, batteries, hotel wastewater) release Cd into the soil[35]. Additionally, the accumulation of Pb, Zn, Cu and Ni in soils is usually associated with traffic emissions[36]. The PERI showed that the study area was at low risk overall, with only point ss04 exhibiting medium risk; however, this result was caused by the abnormally high Cd concentration value (Fig. 4) at point ss04 (Cd (concentration): 1.08 mg/kg, Cd (background): 0.34 mg/kg). This anomalous concentration value has a large influence on the PERI calculated based on the measured concentration, the background value and the toxicity coefficient. Therefore, references to this point can be appropriately removed when considering eco-risk. The PLI of each sampling point was greater than 1 and less than 2, which means that the area was in a moderately contaminated state. In general, the degree of soil HM contamination in this area was low; however, due to HM toxicity, bioaccumulation, and persistence[37], the HM contamination of this area still requires sustained attention.

Correlation analysis is an efficient way to reveal correlations among HMs through Pearson correlation coefficients, and HMs with significant correlations may originate from the same source[38]. As shown in Table S5, the elemental pairs Cd-Cu ($p < 0.01$), Cd-Ni ($p < 0.01$), Cd-Zn ($p < 0.05$), Ni-Cu ($p < 0.01$), Pb—Zn ($p < 0.01$), Cr-Ni ($p < 0.01$), Cr-Pb ($p < 0.05$), Cr-Zn ($p < 0.05$), Zn-Ni ($p < 0.05$), Zn-Cu ($p < 0.01$) were significantly and positively correlated. These results suggest that the elemental group Cd-Cu-Ni-Zn can be considered the same source. The significant correlation of Pb—Zn implies that they have homologous characteristics, and published studies have reported that Pb and Zn are usually enriched by traffic emissions[20]. However, Cr, Ni, Pb and Zn may also share similar sources, and this result is probably caused by mixed sources of HMs, since natural sources, human activities in the study area, or atmospheric deposition may contribute to HM concentrations. Conversely, Cd showed no correlation with Cr and Pb, which indicated that they were controlled by different sources. Therefore,

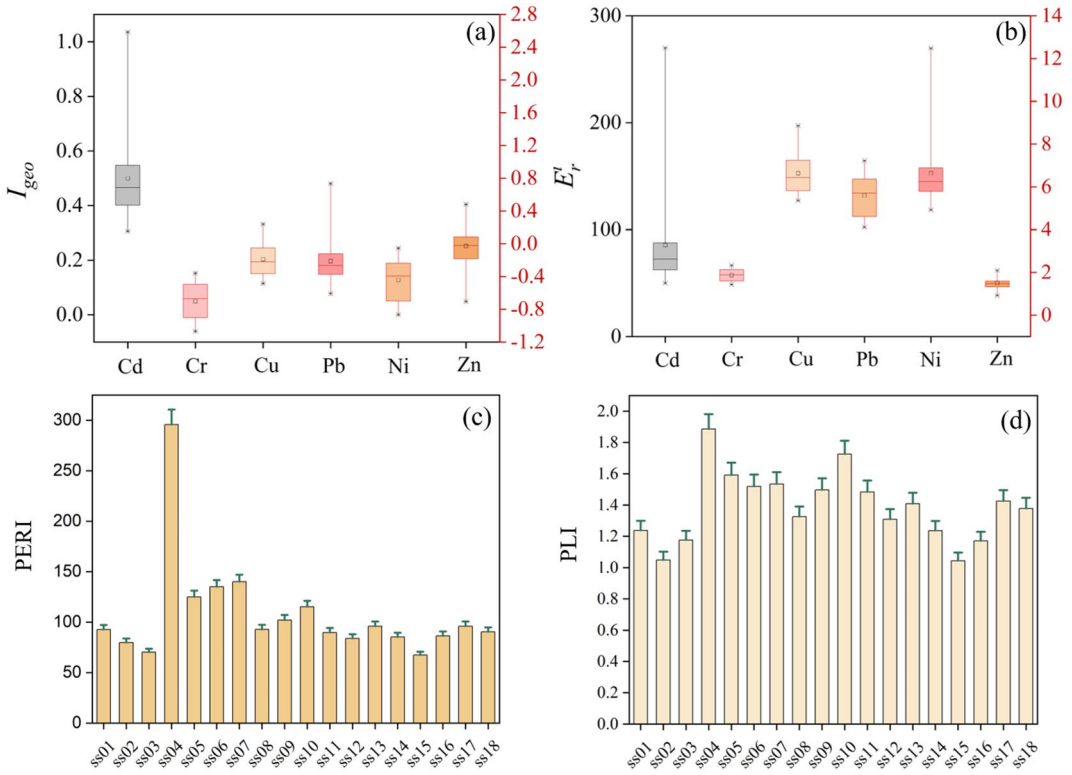

Figure 5. Contamination and ecological risk indices: (**a**) geoaccumulation index (*Igeo*) of HMs; (**b**) ecological risk of individual HMs; (**c**) potential ecological risk index (PERI) of HMs; (**d**) pollution load index (PLI) of HMs.

the PMF model was employed to further identify the sources of HMs and to quantify the contribution of each source to each HM.

The HM concentration data file and uncertainty data file were used as input data according to the EPA PMF5.0 user's guide. To ensure the accuracy and reasonableness of the model results, the factors were set to 2, 3 and 4, and the random starting seed number of the default model was run 100 times. It was determined that the explanatory rate of the model was best with 3 factors. In addition, the coefficient of determination R^2 for all observed and predicted values of HMs was greater than 0.7, with a minimum value of 0.74 and a maximum value of 0.99. Bootstrapping (BS) and displacement of factor elements (DISP) were employed to evaluate the bias and uncertainty of the PMF results[39]. The results showed that over 90% of the base factors were reproduced in the BS model, and no factor swaps were observed in the DISP model within the lowest maximum permitted change in Q (dQ_{max}). Therefore, it is reasonable and valid for the PMF model to explain the information contained in the original data using 3 factors.

The PMF model source apportionment results are shown in Fig. 6, where Factor 1 has high loading values for Pb and Zn (39.7% and 32.0%, respectively), implying that they were influenced by the same sources. The mean concentrations of Pb and Zn exceeded the background values for the tourist area of Sayram Lake, while the CVs were 0.26 and 0.2, respectively, which were medium variation levels, indicating that they might be influenced by human activities[40]. In addition, the I_{geo} indicated the presence of slight level of Pb and Zn contamination at some sampling points in the tourist area of Sayram Lake, which suggests the existence of external sources of Pb and Zn. Published studies have shown that Pb emissions from vehicle exhaust account for two-thirds of total global Pb emissions[41]; despite the global ban on the production and use of leaded gasoline since 2000, vehicle exhaust emissions are still considered to be the main cause of Pb accumulation in soils[42]. Additionally, the wear and tear of brakes, bearings and tires of automobiles also promote the release of Pb and Zn into the soil environment[43]. The soil samples collected in this study were located in the tourist area of Sayram Lake, where tourist visits reach values of 2,530,000 per year and may contribute significantly to local traffic. The frequent vehicle traffic on the G30 highway, emissions from vehicle exhaust and the wear and tear of parts may promote the deposition of Pb and Zn in the topsoil. Therefore, Factor 1 was inferred to be a traffic source.

Factor 2 was dominated by Cr, Cu, Ni, Pb, and Zn, with loadings of 52.2%, 45.8%, 48.9%, 37.1%, and 36.1%, respectively. The average concentration of Cr was lower than the background value, and the average concentrations of Cu and Ni slightly exceeded the local background values. Furthermore, they have small coefficients of variation, indicating low influence from external pollution sources. Notably, Pb and Zn showed high loadings in both Factor 1 and Factor 2, indicating that Pb and Zn were from mixed sources and were controlled by both Factor 1 and Factor 2. Previous studies have shown that Cr, Cu and Ni in soils commonly originate from the soil

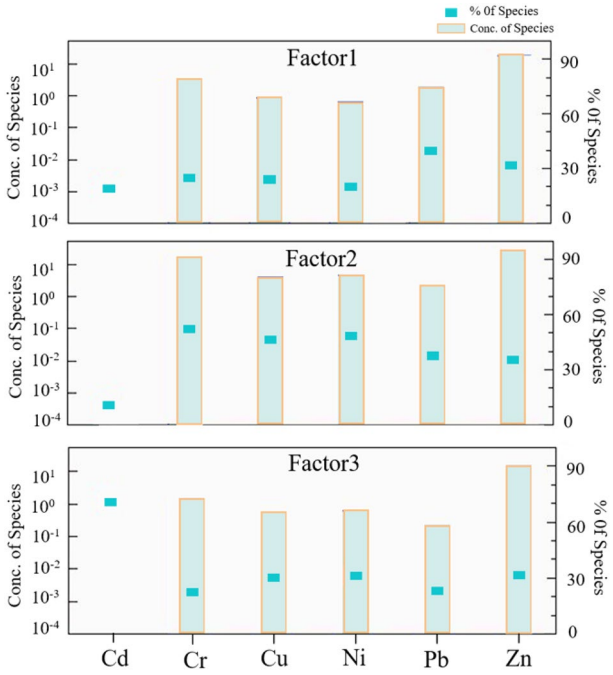

Figure 6. Sources and contributions of HMs in the soil in the PMF model.

parent materials and are controlled by the geological background material and soil-forming processes[44]. Many studies also support this view[45,46]. Therefore, Factor 2 was inferred to be a natural source.

Factor 3 was mainly characterized by Cd, Ni, Cu and Zn, with loadings of 71.1%, 31.0%, 29.9% and 31.9%, respectively. In this study, the mean concentration of Cd was 2.8 times the local soil background value, with a CV of 0.58, which was a strong level of variation in relation to the mean, indicating that Cd may be influenced by anthropogenic sources. According to previous studies, the accumulation of Cd in soils is usually associated with agricultural activities (sewage irrigation, pesticide spraying and fertilizer use)[47], plating of automotive lubricants and brake pads[48], coal combustion[44] and industrial ore smelting[49]. In addition, researchers have found that tourism activities can also increase levels of HMs in soils. In a study conducted by Wang et al.[50] on the effect of tourism activities on soil quality in the scenic area of Mount. Tai, Shandong Province, it was found that tourism activities accelerated the accumulation of HMs, with the average content of Cd exceeding the background value by 36.2%. Enrichment of HMs in soils under tourism loading conditions was also reported in another study, where local soils were highly contaminated with Cd[4]. An investigation of the study area showed that there were no mineral smelting activities or agricultural activities in the basin. The enrichment of Cd may originate from HM-containing wastes from tourism activities (batteries, plastics, wastewater, etc.) and atmospheric deposition (e.g., deposition from the wear and tear from motor vehicles and combustion of coal for heating). Therefore, Factor 3 can be considered a mixed effect of the above sources.

Figure S1 shows the contribution of three factors (F1: traffic source, F2: natural source, F3: tourist waste and atmospheric deposition) to HMs. The contributions of the three factors to Pb and Zn in the soil in a descending order were F1 ≈ F2 > F3. Cr, Cu and Ni were mainly influenced by F2. Cd was controlled by F3 (71.1%). Overall, it seems that the HMs of the topsoil in the tourist area of Sayram Lake were influenced by multiple sources, with the greatest contribution from F2 (38.5%), followed by F3 (34.3%) and F1 (27.2%). Notably, F3 has the greatest capacity to release Cd into the soil environment, and F3 control should be considered a priority.

To validate the results of the PMF model, the sources of Pb in the soil were further analyzed using the Pb isotope method. The Pb isotope ratio results confirmed that the Pb present in the topsoil of the tourist area of Sayram Lake was influenced by anthropogenic sources. As shown in Fig. 7, the Pb isotope ratios in soil samples from the tourist area of Sayram Lake were plotted with those in other related environments ($^{206}Pb/^{207}Pb$ vs. $^{208}Pb/^{206}Pb$). The Pb isotope ratio data of relevant environments mainly include Pb−Zn ores from the Tianshan Mountains in Xinjiang[51], vehicle exhaust emissions in China[52,53], urban road dust in Xinjiang[54] and dustfall in the Tianshan Mountains[55]. Figure 7 shows that there were significant differences in the Pb isotope ratios of different regions. The sampling points near G30 had higher $^{206}Pb/^{207}Pb$ ratios and lower $^{208}Pb/^{206}Pb$ ratios. The sampling points near side roads had lower $^{206}Pb/^{207}Pb$ ratios and higher $^{208}Pb/^{206}Pb$ ratios. The Pb isotope ratios at the sampling sites located near the G30 main road were similar to those of vehicle exhaust emissions, urban road dust and dustfall, and the results indicated that Pb enrichment was strongly related to traffic emissions. Increased human activity has accelerated the accumulation of HMs in the environment, and isotopic methods can identify the sources of HMs based on the similarities they exhibit[14]. By integrating the Pb isotope data in each environment, it was determined that the Pb in the soil of the tourist area of Sayram Lake was partially derived from traffic emissions. This result validated the plausibility of factor 1 in the PMF model being a traffic source.

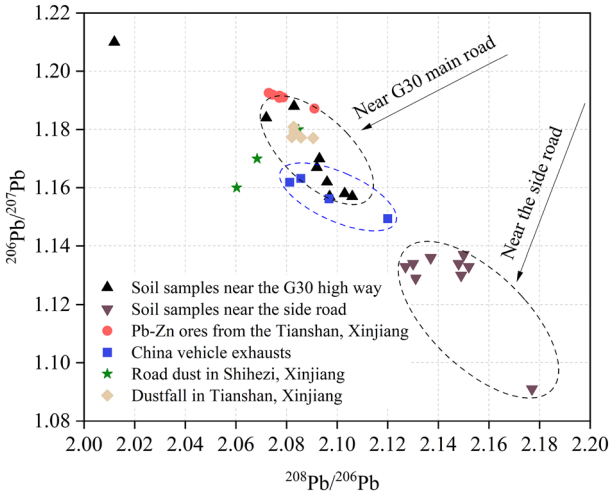

Figure 7. Comparison of Pb isotopic ratios in the topsoil with other relevant studies reported.

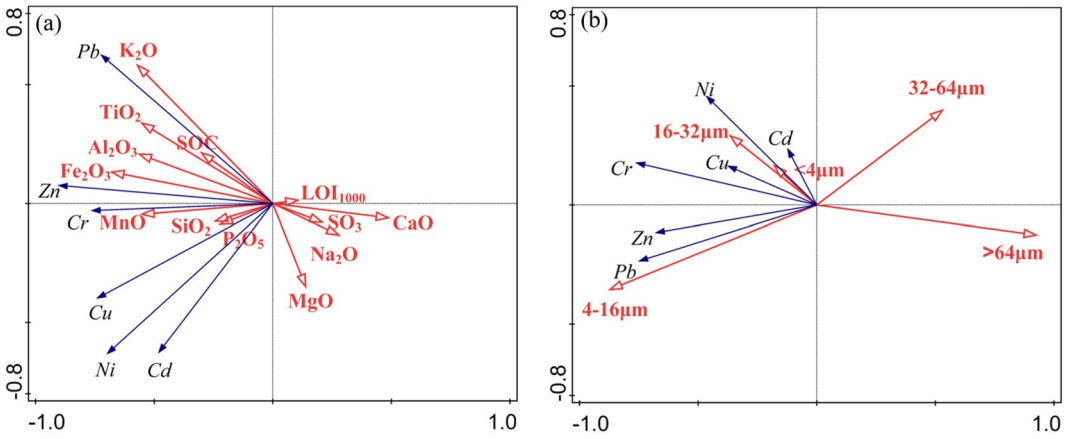

Figure 8. Redundancy analysis of HMs and whole-rock composition, soil organic carbon, and soil grain-size composition.

Study area	Properties	Major pollutants	Driving factors	References
Sayram Lake basin (China)	Tourist area	Cd Pb Zn	Transportation; Tourist waste; Atmospheric deposition;	This study
Dongting lake region (China)	Tourist area	Cd Pb Zn	Transportation; Household waste; Agriculture; Industry	72
Issyk-Kul lake basin (Kyrgyzstan)	Tourist area	Cd Pb Zn	Atmospheric Deposition; Agriculture	73
Bishkek (Kyrgyzstan)	Tourist area	Pb Zn Cu	Transportation	74
Zakopane (Poland)	Tourist town	Cd Zn Pb	Coal combustion; Transportation	75
Gui lin (China)	Tourist town	Pb Zn	Fuel combustion; Transportation	76
Vesuvius (Italy)	National Park	Pb Cu	Transportation	77
Huangshan (China)	National Park	Cd	Transportation	78

Table 1. Comparison of the main pollutants and sources in the topsoil of the Sayram Lake tourist area and other tourist research areas.

A comparison with other tourist areas (Table 1) yielded two distinctive findings: Pb, Zn, Cd and Cu are common pollutants that can easily accumulate in soils in tourism areas; the enrichment of HMs is strongly related to the type of local land use and human activities. Differences in human activities and the geographic contexts of each area lead to differences in the influencing factors and enrichment levels of HMs[56]. To safeguard the soil environmental, HMs that are easily enriched in tourist areas should be highlighted for monitoring, and anthropogenic sources around tourist areas should be reasonably controlled.

The material composition and structure of the soil influence the concentration of HMs in soils. To investigate the effect of soil composition and structure on HMs under natural conditions, data including whole-rock composition, grain size, soil organic carbon and loss-on-ignition were used for redundancy analysis with HMs. Figure 8(a) reveals the relationship between SiO_2, LOI_{1000}, Al_2O_3, CaO, Na_2O, TiO_2, SO_3, P_2O_5, MnO, K_2O, Fe_2O_3, MgO, SOC and Cd, Cr, Cu, Ni, Pb and Zn. The results showed that the content of HMs was related to SiO_2, Al_2O_3, TiO_2, P_2O_5, MnO, K_2O, Fe_2O_3 and SOC. Among them, Pb was most closely related to Al_2O_3 and SOC, and previous studies have shown that soil organic matter has a strong adsorption capacity for HMs[57]. Zn, Cr, Cu and Ni were closely related to Fe–Mn minerals and silicates, which was similar to the results of Ma et al.[58]. Additionally, this also indicated that HMs were weakly affected by carbonate and sulfate. The relationship between HMs and grain size (Fig. 8b) showed that HMs tended to be stored in soil particles with grain sizes < 32 μm. Among them, Cd, Ni, Cu and Cr were associated with clay (< 4 μm) and silt (16–32 μm), while Pb and Zn were associated with a fine-silty (4–16 μm) grade.

The findings revealed that the enrichment of Cd, Pb and Zn in the topsoil of the tourist area of Sayram Lake was influenced by anthropogenic sources. The results of the contamination and eco-risk evaluation suggest that the potential risks posed by the high I_{geo} and E^i_r values of Cd should be treated seriously by relevant authorities. Intensive visitors and traffic will promote the release of HMs that accumulate in the topsoil to contaminate the soil environment and weaken its functions. Tourism quotas have been suggested to reduce soil contamination and degradation[17]. However, for traffic emissions of HMs beyond individual or regional control (e.g., lead in gasoline, car brakes, brake pads and tires), authorities may change their approach and undertake soil remediation. For example, the hyperaccumulation function of plants can be used to reduce HMs in soils or appropriate amounts of soil conditioners can be added[59] to reduce the polluting capacity of HMs by agglomerating them through adsorption and complexation effects.

In this study, the concentration characteristics, potential sources, contamination levels and eco-risk assessment of HMs were analyzed by collecting topsoil samples from the tourist area of Sayram Lake, but some limitations exist. First, a small number of topsoil samples were collected in this study; therefore, they might not adequately reflect the environmental status of the study area and reveal the spatial distribution characteristics of HMs. In addition, the objects of this study only involved Cd, Cr, Cu, Ni, Pb and Zn in the soil, and the absence of studies on other HMs (e.g., Hg, Co, W, etc.) and metalloids (As) has limitations for gaining an overall understanding of the soil environment in this study area. Additionally, HM source apportionment analysis should be combined with multiple source analysis methods to avoid contingency and subjectivity of the results. For example, quantitative analysis methods such as PCA-MLR and CMB can be combined to investigate potential sources and contributions of HMs, and isotope tracing methods for Cd, Cu and Zn can be used to reveal the sources of HMs more accurately. It is worth noting that there are some differences in the pollution evaluation results of the PERI and PLI methods that were caused by the different evaluation standards and thresholds adopted by the different methods. Therefore, the regional applicability of pollution evaluation methods is challenging, and subsequent studies on the toxicological effects of HMs in the region could be carried out to determine the pollution evaluation criteria and thresholds suitable for this region.

Conclusions

This study examined Cd, Cr, Cu, Ni, Pb and Zn in the topsoils of the Sayram Lake tourist area in Xinjiang, discussed their concentration characteristics, contamination levels, eco-risk characteristics and potential sources, and reached the following conclusions:

1. Cd, Pb and Zn were generally enriched in the topsoil, and their mean concentrations were 2.83, 1.33, and 1.5 times higher than the local background values, respectively. In contrast, the average concentrations of Cr, Cu and Ni were close to the corresponding background values.
2. The calculated I_{geo} and E^i_r indicated that the topsoil was more severely contaminated with Cd. The PERI suggested that the eco-risk in this study area was low, and the PLI in the tourist area of Sayram Lake ranged from 1.04 to 1.89, with a mean value of 1.39, indicating a moderate contamination level.
3. Three sources of soil HMs were identified and apportioned by combining the PMF model and Pb isotope ratios, namely, traffic sources (27.2%), natural sources (38.5%), and mixed sources (tourism waste and atmospheric deposition) (34.3%). The source apportionment results showed that Cr, Cu, and Ni were mainly derived from natural sources, Pb and Zn were attributed to traffic sources and natural sources, and Cd was associated with tourist wastes and atmospheric deposition.
4. The utilization of whole-rock composition and grain size data of the soils was an efficient way to study the influencing factors for HMs. The content of HMs in the topsoil of the tourist area of Sayram Lake was influenced by SiO_2, Al_2O_3, TiO_2, P_2O_5, MnO, K_2O, Fe_2O_3 and SOC. Additionally, the content of HMs was also influenced by soil grain size, and HMs tended to be stored in soil particles with grain sizes < 32 μm.

Materials and methods

Geographical setting. The Sayram Lake Basin (Fig. 1) is located on the northern slope of the Tianshan Mountains and in the hinterland of the Eurasian continent. The basin belongs to Bole city, adjacent to Wenquan County, Horgos city, Huocheng County and Yining County, with a drainage area of 1408 km^2 [60]. The area has a temperate alpine climate type, with an annual average temperature and an annual average precipitation of 0.5 °C and 350 mm, respectively[61].

The vegetation type of the Sayram Lake watershed is relatively homogeneous, with the lake area making up 24.8% of the watershed area, and the rest of the land is mainly covered by high-, medium- and low-coverage grassland (59.6%), woodland (5.2%), bare rock (8.7%), and Gobi (1.5%) compositions (Fig. 1). The tourist area of Sayram Lake is popular among tourists, with an average daily admission of nearly 7,000 visitors. The G30 highway runs along the southeast side of Sayram Lake through the basin to bring superior transportation conditions, while the construction of a 79 km-long tourist road around the lake promotes tourism.

Sample collection. To study the accumulation of HMs caused by human activities in Sayram Lake Basin, sampling sites were predefined in this study based on the traffic deployment in the Sayram Lake watershed and the activity areas of tourists in this tourist area. In total, 18 topsoil samples were collected from the study area, and topsoil samples were collected from 0–20 cm in October 2020, and GPS was used for geographic positioning. To prevent the topsoil samples from becoming cross-contaminated, the collected topsoil samples were immediately placed in polyethylene bags and sealed for storage. The stainless-steel drill bit was cleaned between samples.

Sample preparation and laboratory analysis. Soil samples collected in the field were naturally dried at room temperature in the laboratory. Then, impurities were removed from the soil samples, and the soil was crushed using an agate mortar and passed through a 200-mesh nylon sieve. The processed soil samples were sealed in polyethylene bags for further chemical analysis. The determination and analysis of HMs and whole-rock, organic carbon and Pb isotopes in the soil samples were performed at ALS Minerals-ALS Chemex (Guangzhou, China).

The soil samples (0.125 g) were digested in three stages using HCl-HNO_3-HF-$HClO_4$. First, HNO_3 and $HClO_4$ were used for preoxidation. Then, HF was added, and the mixture was heated in an electric furnace. Finally, the remaining solution was diluted with HCl. The concentrations of Cr, Cu, Ni, Pb and Zn were determined by inductively coupled plasma atomic emission spectroscopy (ICP−AES) (Agilent, 5110, USA). The concentrations of Cd were determined by inductively coupled plasma−mass spectrometry (ICP−MS) (Agilent, 7900, USA).

An X-ray fluorescence spectrometer (PANalytical, PW2424, Netherlands) was used to analyze the whole-rock composition of the soil, and the ME-XRF26 method provided by ALS Minerals-ALS Chemex (Guangzhou, China) was applied to determine the Al_2O_3, CaO, Fe_2O_3, K_2O, MgO, MnO, Na_2O, P_2O_5, SiO_2, SO_3 and TiO_2 content percentages. The loss-on-ignition of soil samples was determined based on the OA-GRA05x method provided by ALS Minerals-ALS Chemex (Guangzhou, China) at 1000 °C (LOI_{1000}). The detection limit for loss-on-ignition was 0.01%, and the relative deviation and relative error of the method were both less than 5%. A carbon–sulfur analyzer (LECO, CS844, USA) was used for soil organic carbon analysis. The soil samples that were digested by HCl were separated and filtered for organic carbon with a porous crucible. The crucible was cleaned with deionized water, dried and placed in an infrared induction furnace to quantitatively detect the percentage content of soil organic carbon. The detection limit for soil organic carbon was 0.02%, and the relative deviation and relative error of the method were less than 5% and 3.5%, respectively.

The Pb isotope ratios ($^{208}Pb/^{206}Pb$ and $^{207}Pb/^{206}Pb$) of the digested soil were determined by ICP−MS (Agilent 7700x), and the instrument was calibrated using a reference material (SRM981-NIST, USA) and standard material (GBW04426, China) for quality control. The relative standard deviations (RSD) of $^{208}Pb/^{206}Pb$ and $^{207}Pb/^{206}Pb$ were less than 0.02 for multiple measurements of the reference material GBW04426.

Soil grain size was measured by a Bettersizer laser grain-size analyzer (BT-9300SE) manufactured in China, and the measurement accuracy error and repeatability error were both less than 1%. According to the Udden-Wentworth[33] grain size classification standard, the soil grain size in this study included clay (< 4 μm), fine-silty (4–16 μm), silt (16–32 μm), coarse-silty (32–64 μm) and sandy (> 64 μm) grades.

Quality assurance and quality control. To ensure the accuracy of the experimental data, monitoring materials (blank samples, duplicate samples and standard materials (MRGeo08, GBW07179) were inserted in each testing batch for HM testing of soil samples. The detection limits for HMs (Cr, Cu, Ni, Zn, Pb and Cd) were 1 mg/kg, 0.2 mg/kg, 0.2 mg/kg, 2 mg/kg, 0.5 mg/kg and 0.02 mg/kg, respectively, and the analytical errors were less than 5%. The limits of detection for whole-rock compositions (Al_2O_3, CaO, Fe_2O_3, K_2O, MgO, MnO, Na_2O, P_2O_5, SiO_2, SO_3 and TiO_2) were 0.01%, and the analytical errors were less than 5%.

Statistical analysis methods. In this study, R 4.0.4 software was used for descriptive statistics, descriptive data such as the mean, maximum and minimum values, and coefficient of variation (CV) were calculated, and Pearson correlation analysis was used for preliminary source analysis. Origin 2021b software was used to map the whole-rock composition and particle size characteristics, elemental concentration characteristics, ecological risk assessment results and comparative Pb isotopes of the soil samples. Canoco5[62] was applied to complete redundancy analysis between HMs and whole-rock elements and grain size.

Ecological risk assessment methods. (1) Geoaccumulation index (I_{geo})**.** To assess the degree of HM contamination in the topsoil of the tourist area of Sayram Lake, I_{geo} was used as an indicator for evaluation, and it was defined as follows[63]:

$$I_{geo} = \log_2\left(\frac{C_i}{1.5 * B_i}\right) \tag{1}$$

where C_i represents the measured concentration value of element *i*, and *Bi* represents the local background value of element *i*. The background values of HMs in this study were referenced from the 1994 statistics of the China National Environmental Monitoring Centre[64] in the Sayram Lake Basin (Cd: 0.12, Cr: 57.3, Cu: 20.7, Ni: 24.9, Pb: 18.5, Zn: 67.3, Unit: mg/kg). I_{geo} is divided into 7 categories[65], indicating different levels of contamination, and the classification information is presented in Table S3.

(2) Pollution load index (PLI). The PLI method was originally developed by Tomlinson et al. and is now widely used for soil HM contamination assessment[66]. The calculation is as follows:

$$CF_i = \frac{C_i}{B_i} \tag{2}$$

$$PLI = (CF_1 * CF_2 * CF_3 * \cdots * CF_n)^{\frac{1}{n}} \tag{3}$$

where CF_i represents the pollution index value of a single factor, *Ci* denotes the measured concentration of pollutant *i* and *Bi* refers to the background value of element *i*. A PLI less than 1 indicates no contamination, and a PLI greater than 1 and less than 2 indicates moderate contamination.

(3) Potential ecological risk index (PERI). The PERI method was originally developed by Hakanson[67], it integrates the ecological and toxicological effects of HMs, and it is widely used for the assessment of the eco-risk and contamination levels of the soil environment by HMs[68].

$$C_r^i = \frac{C_i}{B_i} \tag{4}$$

$$E_r^i = T_i * C_r^i \tag{5}$$

$$PERI = \sum_{i=1}^{n} E_r^i \tag{6}$$

where C_i denotes the measured concentration of pollutant *i*, B_i denotes the background concentration of element *i*, *Ci r* denotes the enrichment coefficient of the element, E^i_r denotes the eco-risk of the individual pollutant, and T_i represents the toxicity coefficient, which was derived from a previously published study for Cd, Cr, Cu, Ni, Pb, and Zn (the values were 30, 2, 5, 5, 5, and 1, respectively)[69]. PERI is classified into 4 risk levels, ranging from low risk to significantly high risk (Table S4).

Positive matrix factorization (PMF). The PMF model is a receptor model recommended by the US EPA for source analysis of environmental pollutants[70,71], which was used in this study for source analysis of HMs in the tourist area of Sayram Lake. The basic equation of the PMF receptor model is as follows:

$$X_{ij} = \sum_{k=1}^{p} \left(g_{ik} f_{kj} + e_{ij}\right) \tag{7}$$

where X_{ij} denotes the measured concentration of HM *j* in sample *i*, g_{ik} denotes the contribution of the *k*th source to the *i*th sample, f_{ik} represents the eigenvalue of contamination source *k* to the j_{th} HM concentration, and e_{ij} is the residual matrix. The optimal matrix of *g* and *f* can be obtained by continuously minimizing the objective function *Q*. The calculation of Q is as follows:

$$Q = \sum_{i=1}^{n} \sum_{j=1}^{m} \left(\frac{e_{ij}}{u_{ij}}\right)^2 \tag{8}$$

where u_{ij} is the uncertainty, and its calculation depends on whether the concentration of HMs is lower than the method detection limit (MDL). When the concentration of HMs exceeds the MDL, u_{ij} can be calculated according to the following equation:

$$u_{ij} = \sqrt{\left(error\ fraction * c\right)^2 + MDL^2} \tag{9}$$

Otherwise, u_{ij} is calculated by the following equation:

$$u_{ij} = 5/6 * MDL \tag{10}$$

where *c* is the concentration of the HMs, MDL denotes the method detection limit, and the error fraction is the percentage of measurement uncertainty.

Data availability

The datasets generated and/or analyzed during the current study are not publicly available because the data are a part of an ongoing study, but they are available from the corresponding author on reasonable request.

Received: 17 August 2022; Accepted: 9 November 2022
Published online: 12 November 2022

References

1. Zhang, H. *et al.* Pollutant source, ecological and human health risks assessment of heavy metals in soils from coal mining areas in Xinjiang, China. *Environ. Res.* **202**, 111702. https://doi.org/10.1016/j.envres.2021.111702 (2021).
2. Zhang, X. *et al.* Impact of soil heavy metal pollution on food safety in China. *PLoS ONE* **10**(8), e0135182. https://doi.org/10.1371/journal.pone.0135182 (2015).
3. Yuan, G. *et al.* Source identification and ecological risk assessment of heavy metals in topsoil using environmental geochemical mapping: typical urban renewal area in Beijing, China. *J. Geochem. Explor.* **136**, 40–47. https://doi.org/10.1016/j.gexplo.2013.10.002 (2014).
4. Ciarkowska, K. Assessment of heavy metal pollution risks and enzyme activity of meadow soils in urban area under tourism load: a case study from Zakopane (Poland). *Environ. Sci. Pollut. Res.* **25**(14), 13709–13718. https://doi.org/10.1007/s11356-018-1589-y (2018).
5. Chen, T.-B. *et al.* Assessment of heavy metal pollution in surface soils of urban parks in Beijing, China. *Chemosphere* **60**(4), 542–551. https://doi.org/10.1016/j.chemosphere.2004.12.072 (2005).
6. Wu, Q. *et al.* Spatial distribution, ecological risk and sources of heavy metals in soils from a typical economic development area, Southeastern China. *Sci. Total Environ.* **780**, 146557. https://doi.org/10.1016/j.scitotenv.2021.146557 (2021).
7. Fang, L. *et al.* Proper land use for heavy metal-polluted soil based on enzyme activity analysis around a Pb-Zn mine in Feng County, China. *Environ. Sci. Pollut. Res.* **24**(36), 28152–28164. https://doi.org/10.1007/s11356-017-0308-4 (2017).
8. De Miguel, E. *et al.* Risk-based evaluation of the exposure of children to trace elements in playgrounds in Madrid (Spain). *Chemosphere* **66**(3), 505–513. https://doi.org/10.1016/j.chemosphere.2006.05.065 (2007).
9. Yang, S. *et al.* Status assessment and probabilistic health risk modeling of metals accumulation in agriculture soils across China: A synthesis. *Environ. Int.* **128**, 165–174. https://doi.org/10.1016/j.envint.2019.04.044 (2019).
10. Yan, L., Franco, A.-M. & Elio, P. Health risk assessment via ingestion and inhalation of soil PTE of an urban area. *Chemosphere* **281**, 130964. https://doi.org/10.1016/j.chemosphere.2021.130964 (2021).
11. Le Roux, G., Hansson, S. V. & Claustres, A. Inorganic chemistry in the mountain critical zone: are the mountain water towers of contemporary society under threat by trace contaminants? In *Developments in Earth Surface Processes* 131–154 (Elsevier, 2016).
12. Le Roux, G. *et al.* Trace metal legacy in mountain environments: a view from the Pyrenees Mountains. In *Biogeochemical Cycles: Ecological Drivers Environmental Impact* (eds Dontsova, K. *et al.*) 191–206 (Wiley, 2020). https://doi.org/10.1002/9781119413332.ch9.
13. Lv, J. & Wang, Y. PMF receptor models and sequential Gaussian simulation to determine the quantitative sources and hazardous areas of potentially toxic elements in soils. *Geoderma* **353**, 347–358. https://doi.org/10.1016/j.geoderma.2019.07.020 (2019).
14. Bing, H. *et al.* Vegetation and cold trapping modulating elevation-dependent distribution of trace metals in soils of a high mountain in eastern Tibetan Plateau. *Sci. Rep.* **6**(1), 1–14. https://doi.org/10.1038/srep24081 (2016).
15. Yang, Q. *et al.* A review of soil heavy metal pollution from industrial and agricultural regions in China: Pollution and risk assessment. *Sci. Total Environ.* **642**, 690–700. https://doi.org/10.1016/j.scitotenv.2018.06.068 (2018).
16. Zhang, H. *et al.* Identification of traffic-related metals and the effects of different environments on their enrichment in roadside soils along the Qinghai-Tibet highway. *Sci. Total Environ.* **521**, 160–172. https://doi.org/10.1016/j.scitotenv.2015.03.054 (2015).
17. Brtnický, M. *et al.* The impact of tourism on extremely visited volcanic island: Link between environmental pollution and transportation modes. *Chemosphere* **249**, 126118. https://doi.org/10.1016/j.chemosphere.2020.126118 (2020).
18. Azam, M., Alam, M. M. & Hafeez, M. H. Effect of tourism on environmental pollution: Further evidence from Malaysia, Singapore and Thailand. *J. Clean. Prod.* **190**, 330–338. https://doi.org/10.1016/j.jclepro.2018.04.168 (2018).
19. Huang, J. *et al.* A new exploration of health risk assessment quantification from sources of soil heavy metals under different land use. *Environ. Pollut.* **243**, 49–58. https://doi.org/10.1016/j.envpol.2018.08.038 (2018).
20. Jiang, H. *et al.* An integrated exploration on health risk assessment quantification of potentially hazardous elements in soils from the perspective of sources. *Ecotoxicol. Environ. Saf.* **208**, 111489. https://doi.org/10.1016/j.ecoenv.2020.111489 (2021).
21. Li, Y. *et al.* Health risk of heavy metal exposure from dustfall and source apportionment with the PCA-MLR model: A case study in the Ebinur Lake Basin, China. *Atmos. Environ.* **272**, 118950. https://doi.org/10.1016/j.atmosenv.2022.118950 (2022).
22. Guan, Q. *et al.* Source apportionment of heavy metals in farmland soil of Wuwei, China: Comparison of three receptor models. *J. Clean. Prod.* **237**, 117792. https://doi.org/10.1016/j.jclepro.2019.117792 (2019).
23. Chen, Z. *et al.* Combination of UNMIX, PMF model and Pb-Zn-Cu isotopic compositions for quantitative source apportionment of heavy metals in suburban agricultural soils. *Ecotoxicol. Environ. Saf.* **234**, 113369. https://doi.org/10.1016/j.ecoenv.2022.113369 (2022).
24. Gao, B. *et al.* Cd isotopes as a potential source tracer of metal pollution in river sediments. *Environ. Pollut.* **181**, 340–343. https://doi.org/10.1016/j.envpol.2013.05.048 (2013).
25. Jiang, H. *et al.* An integrated approach to quantifying ecological and human health risks from different sources of soil heavy metals. *Sci. Total Environ.* **701**, 134466. https://doi.org/10.1016/j.scitotenv.2019.134466 (2020).
26. Jiang, Y. *et al.* Source apportionment and health risk assessment of heavy metals in soil for a township in Jiangsu Province, China. *Chemosphere* **168**, 1658–1668. https://doi.org/10.1016/j.chemosphere.2016.11.088 (2017).
27. Amil, N. *et al.* Seasonal variability of PM 2.5 composition and sources in the Klang Valley urban-industrial environment. *Atmos. Chem.* **16**(8), 5357–5381. https://doi.org/10.5194/acp-16-5357-2016 (2016).
28. Xu, M. *et al.* Detection of spatio-temporal variability of air temperature and precipitation based on long-term meteorological station observations over Tianshan Mountains, Central Asia. *Atmos. Res.* **203**, 141–163. https://doi.org/10.1016/j.atmosres.2017.12.007 (2018).
29. Chen, Y. *et al.* Impact of climate change on water resources in the Tianshan Mountians. *Acta Geogr. Sin.* **72**(1), 18–26. https://doi.org/10.3969/j.issn.0371-5736.2012 (2017).
30. Wei, H. *et al.* Spatial–temporal variation of land use and land cover change in the glacial affected area of the Tianshan Mountains. *CATENA* **202**, 105256. https://doi.org/10.1016/j.catena.2021.105256 (2021).
31. Tang, Z. *et al.* Spatiotemporal variation of snow cover in Tianshan Mountains, Central Asia, based on cloud-free MODIS fractional snow cover product, 2001–2015. *Remote Sens.* **9**(10), 1045. https://doi.org/10.3390/rs9101045 (2017).

32. Liu, W. *et al.* A 200-year sediment record of environmental change from Lake Sayram, Tianshan Mountains in China. *GFF* **136**(4), 548–555. https://doi.org/10.1080/11035897.2014.918170 (2014).
33. Blair, T. C. & McPherson, J. G. Grain-size and textural classification of coarse sedimentary particles. *J. Sediment. Res.* **69**(1), 6–19 (1999).
34. Zhong, X. *et al.* Factors influencing heavy metal availability and risk assessment of soils at typical metal mines in Eastern China. *J. Hazard. Mater.* **400**, 123289. https://doi.org/10.1016/j.jhazmat.2020.123289 (2020).
35. Sharma, A. & Uniyal, S. K. Heavy metal accumulation in *Pyrrosia flocculosa* (D. Don) Ching growing in sites located along a vehicular disturbance gradient. *Environ. Monit. Assess.* **188**(10), 1–12. https://doi.org/10.1007/s10661-016-5561-3 (2016).
36. Wang, J. *et al.* Health risk assessment of heavy metal (loid) s in the farmland of megalopolis in China by using APCS-MLR and PMF receptor models: Taking Huairou District of Beijing as an example. *Sci. Total Environ.* **835**, 155313. https://doi.org/10.1016/j.scitotenv.2022.155313 (2022).
37. Zhang, J., Hua, P. & Krebs, P. Influences of land use and antecedent dry-weather period on pollution level and ecological risk of heavy metals in road-deposited sediment. *Environ. Pollut.* **228**, 158–168. https://doi.org/10.1016/j.envpol.2017.05.029 (2017).
38. Cai, L. *et al.* Heavy metals in agricultural soils from a typical township in Guangdong Province, China: Occurrences and spatial distribution. *Ecotoxicol. Environ. Saf.* **168**, 184–191. https://doi.org/10.1016/j.ecoenv.2018.10.092 (2019).
39. Yuanan, H. *et al.* Quantitative source apportionment of heavy metal (loid) s in the agricultural soils of an industrializing region and associated model uncertainty. *J. Hazard. Mater.* **391**, 122244. https://doi.org/10.1016/j.jhazmat.2020.122244 (2020).
40. Guan, Q. *et al.* Source apportionment of heavy metals in agricultural soil based on PMF: A case study in Hexi Corridor, northwest China. *Chemosphere* **193**, 189–197. https://doi.org/10.1016/j.chemosphere.2017.10.151 (2018).
41. Fei, X. *et al.* Contamination assessment and source apportionment of heavy metals in agricultural soil through the synthesis of PMF and GeogDetector models. *Sci. Total Environ.* **747**, 1412. https://doi.org/10.1016/j.scitotenv.2020.141293 (2020).
42. Chen, T. *et al.* Identification of soil heavy metal sources and improvement in spatial mapping based on soil spectral information: A case study in northwest China. *Sci. Total Environ.* **565**, 155–164. https://doi.org/10.1016/j.scitotenv.2016.04.163 (2016).
43. Chang, X. *et al.* Refining the diagnostics of non-point source metals pollution to urban lakes based on interaction normalized PMF coupled with Bayesian network. *Environ. Pollut.* **304**, 119194. https://doi.org/10.1016/j.envpol.2022.119194 (2022).
44. Sun, L. *et al.* Levels, sources, and spatial distribution of heavy metals in soils from a typical coal industrial city of Tangshan, China. *CATENA* **175**, 101–109. https://doi.org/10.1016/j.catena.2018.12.014 (2019).
45. Liang, J. *et al.* Spatial distribution and source identification of heavy metals in surface soils in a typical coal mine city, Lianyuan, China. *Environ. Pollut.* **225**, 681–690. https://doi.org/10.1016/j.envpol.2017.03.057 (2017).
46. Zhang, X. *et al.* Source identification and spatial distribution of arsenic and heavy metals in agricultural soil around Hunan industrial estate by positive matrix factorization model, principle components analysis and geo statistical analysis. *Ecotoxicol. Environ. Saf.* **159**, 354–362. https://doi.org/10.1016/j.ecoenv.2018.04.072 (2018).
47. Hu, Y., Cheng, H. & Tao, S. The challenges and solutions for cadmium-contaminated rice in China: a critical review. *Environ. Int.* **92**, 515–532. https://doi.org/10.1016/j.envint.2016.04.042 (2016).
48. McKenzie, E. R. *et al.* Metals associated with stormwater-relevant brake and tire samples. *Sci. Total Environ.* **407**(22), 5855–5860. https://doi.org/10.1016/j.scitotenv.2009.07.018 (2009).
49. Liao, J. *et al.* Heavy metals in river surface sediments affected with multiple pollution sources, South China: Distribution, enrichment and source apportionment. *J. Geochem. Explor.* **176**, 9–19. https://doi.org/10.1016/j.gexplo.2016.08.013 (2017).
50. Wang, J., Dong, Y. & Liu, C. Impacts of tourism activities on soil quality of mountain Tai scenic area. *Acta Pedol. Sin. (China)* **49**(2), 398–402 (2012) (**(In Chinese)**).
51. Gao, R. *et al.* Source and possible leaching process of ore metals in the Uragen sandstone-hosted Zn-Pb deposit, Xinjiang, China: Constraints from lead isotopes and rare earth elements geochemistry. *Ore Geol. Rev.* **106**, 56–78. https://doi.org/10.1016/j.oregeorev.2019.01.012 (2019).
52. Tan, M. *et al.* Comprehensive study of lead pollution in Shanghai by multiple techniques. *Anal. Chem.* **78**(23), 8044–8050. https://doi.org/10.1021/ac061365q (2006).
53. Zhu, B., Chen, Y. & Peng, J.-H. Lead isotope geochemistry of the urban environment in the Pearl River Delta. *Appl. Geochem.* **16**(4), 409–417. https://doi.org/10.1016/S0883-2927(00)00047-0 (2001).
54. Huang, Y. *et al.* Lead Pollution and Isotopic Signature of the Dusts around Urban Roads in Shihezi City, Xinjiang Province. *Rock Miner. Anal.* **32**(4), 632–637. https://doi.org/10.3969/j.issn.0254-5357.2013.04.020 (2013).
55. Nagatsuka, N. *et al.* Sr, Nd and Pb stable isotopes of surface dust on Ürümqi glacier No. 1 in western China. *Ann. Glaciol.* **51**(56), 95–105. https://doi.org/10.3189/172756411795931895 (2010).
56. Liu, L. *et al.* Heavy metal (loid) s in the topsoil of urban parks in Beijing, China: Concentrations, potential sources, and risk assessment. *Environ. Pollut.* **260**, 114083. https://doi.org/10.1016/j.envpol.2020.114083 (2020).
57. Yin, Y. *et al.* The importance of organic matter distribution and extract soil: solution ratio on the desorption of heavy metals from soils. *Sci. Total Environ.* **287**(1–2), 107–119. https://doi.org/10.1016/S0048-9697(01)01000-2 (2002).
58. Ma, L., Abuduwaili, J. & Liu, W. Spatial distribution and ecological risks of the potentially-toxic elements in the surface sediments of Lake Bosten, China. *Toxics* **8**(3), 77. https://doi.org/10.3390/toxics8030077 (2020).
59. Mohammed, A. S., Kapri, A. & Goel, R. Heavy metal pollution: source, impact, and remedies. In *Biomanagement of metal-contaminated soils* 1–28 (Springer, 2011).
60. Wang, S. & Dou, H. *Chinese Lake Chronicles* (Science Press, 1998).
61. Zeng, H., Wu, J. & Liu, W. Two-century sedimentary record of heavy metal pollution from Lake Sayram: A deep mountain lake in central Tianshan, China. *Quat. Int.* **321**, 125–131. https://doi.org/10.1016/j.quaint.2013.09.047 (2014).
62. Braak, T. & Smilauer, P. *Canoco Reference Manual and User's Guide: Software for Ordination, Version 5.0* 1–496 (Microcomputer Power Press, 2012).
63. Wang, N. *et al.* Calculation and application of Sb toxicity coefficient for potential ecological risk assessment. *Sci. Total Environ.* **610**, 167–174. https://doi.org/10.1016/j.scitotenv.2017.07.268 (2018).
64. Zheng, C. *The Atlas of Soil Environment Background Value in the People's Republic of China* (China Environmental Science Press, 1994).
65. Feng, Y., Chenglin, L. & Bowen, W. Evaluation of heavy metal pollution in the sediment of Poyang Lake based on stochastic geo-accumulation model (SGM). *Sci. Total Environ.* **659**, 1–6. https://doi.org/10.1016/j.scitotenv.2018.12.311 (2019).
66. Tian, K. *et al.* Ecological risk assessment of heavy metals in sediments and water from the coastal areas of the Bohai Sea and the Yellow Sea. *Environ. Int.* **136**, 105512. https://doi.org/10.1016/j.envint.2020.105512 (2020).
67. Hakanson, L. An ecological risk index for aquatic pollution control. A sedimentological approach. *Water Res.* **14**(8), 975–1001. https://doi.org/10.1016/0043-1354(80)90143-8 (1980).
68. Men, C. *et al.* Source-specific ecological risk analysis and critical source identification of heavy metals in road dust in Beijing, China. *J. Hazard. Mater.* **388**, 121763. https://doi.org/10.1016/j.jhazmat.2019.121763 (2020).
69. Xu, Z. Q. *et al.* Calculation of heavy metals' toxicity coefficient in the evaluation of potential ecological risk index. *Environ. Sci. Technol.* **31**(2), 112–115. https://doi.org/10.3969/j.issn.1003-6504.2008.02.030 (2008).
70. Paatero, P. & Tapper, U. Positive matrix factorization: A non-negative factor model with optimal utilization of error estimates of data values. *Environmetrics* **5**(2), 111–126. https://doi.org/10.1002/env.3170050203 (1994).

71. Chai, L. *et al.* Quantitative source apportionment of heavy metals in cultivated soil and associated model uncertainty. *Ecotoxicol. Environ. Saf.* **215**, 112150. https://doi.org/10.1016/j.ecoenv.2021.112150 (2021).
72. Zhang, Y. *et al.* Heavy metals in soils and sediments from Dongting Lake in China: occurrence, sources, and spatial distribution by multivariate statistical analysis. *Environ. Sci. Pollut. Res.* **25**(14), 13687–13696. https://doi.org/10.1007/s11356-018-1590-5 (2018).
73. Ma, L. *et al.* Controlling factors and pollution assessment of potentially toxic elements in topsoils of the Issyk-Kul Lake region, Central Asia. *Soil Sedim. Contam. Int. J.* **27**(2), 147–160. https://doi.org/10.1080/15320383.2018.1433632 (2018).
74. Ma, L. *et al.* Anthropogenically disturbed potentially toxic elements in roadside topsoils of a suburban region of Bishkek, Central Asia. *Soil Use Manag.* **35**(2), 283–292. https://doi.org/10.1111/sum.12470 (2019).
75. Ciarkowska, K. *et al.* Polycyclic aromatic hydrocarbon and heavy metal contents in the urban soils in southern Poland. *Chemosphere* **229**, 214–226. https://doi.org/10.1016/j.chemosphere.2019.04.209 (2019).
76. Shahab, A. *et al.* Pollution characteristics and toxicity of potentially toxic elements in road dust of a tourist city, Guilin, China: Ecological and health risk assessment☆. *Environ. Pollut.* **266**, 115419. https://doi.org/10.1016/j.envpol.2020.115419 (2020).
77. Memoli, V. *et al.* Seasonality, altitude and human activities control soil quality in a national park surrounded by an urban area. *Geoderma* **337**, 1–10. https://doi.org/10.1016/j.geoderma.2018.09.009 (2019).
78. Huang, J. *et al.* Do trace metal (loid) s in road soils pose health risks to tourists? A case of a highly-visited national park in China. *J. Environ. Sci.* **111**, 61–74. https://doi.org/10.1016/j.jes.2021.02.032 (2022).

Acknowledgements

This research is funded by the National Natural Science Foundation of China (U1903115), LU JIAXI International team program supported by the K.C. Wong Education Foundation (GJTD-2020-14), and the High-level Training Project of Xinjiang Institute of Ecology and Geography, CAS (E050030101).

Author contributions

T.Z. conceived the idea of the study and designed the research, wrote the paper, discussed the results and revised the manuscript. L.M. conceived the idea of the study and designed the research, discussed the results and revised the manuscript; and were involved in funding acquisition and supervision. J.A. and W.L. discussed the results and revised the manuscript. Y.L. and S.F. was involved in part of the experimental analysis, analyzed the partial data, discussed the results and revised the manuscript.

Competing interests

The authors declare no competing interests.

Additional information

Supplementary Information The online version contains supplementary material available at https://doi.org/10.1038/s41598-022-24064-1.

Correspondence and requests for materials should be addressed to L.M.

Reprints and permissions information is available at www.nature.com/reprints.

Publisher's note Springer Nature remains neutral with regard to jurisdictional claims in published maps and institutional affiliations.